Liquid Crystals
Publication details, including instructions for authors and subscription information:
http://www.informaworld.com/smpp/title~content=t713926090

Overall analysis of first-order phase transitions in some alkyloxycyanobiphenyl liquid crystals

P. Cusmin[a]; J. Salud[a]; D. O. López[a]; S. Diez-Berart[ab]; M. R. de la Fuente[c]; M. A. Pérez-Jubindo[c]; N. Veglio[a]
[a] Laboratori de Caracterització de Materials (LCM-GPFM), Departament de Física i Enginyeria Nuclear, ETSEIB Universitat Politècnica de Catalunya, 647 08028 Barcelona, Spain [b] Liquid Crystals Institute, Kent State University, Kent, USA [c] Departamento de Física Aplicada II, Facultad de Ciencias, Universidad del País Vasco, E-48080 Bilbao, Spain

To cite this Article Cusmin, P. , Salud, J. , López, D. O. , Diez-Berart, S. , de la Fuente, M. R. , Pérez-Jubindo, M. A. and Veglio, N.(2008) 'Overall analysis of first-order phase transitions in some alkyloxycyanobiphenyl liquid crystals', Liquid Crystals, 35: 6, 695 — 703

To link to this Article: DOI: 10.1080/02678290802120273

URL: http://dx.doi.org/10.1080/02678290802120273

Liquid Crystals,
Vol. 35, No. 6, June 2008, 695–703

Overall analysis of first-order phase transitions in some alkyloxycyanobiphenyl liquid crystals

P. Cusmin[a], J. Salud[a]*, D. O. López[a], S. Diez-Berart[ab], M. R. de la Fuente[c], M. A. Pérez-Jubindo[c] and N. Veglio[a]

[a]*Laboratori de Caracterització de Materials (LCM-GPFM), Departament de Física i Enginyeria Nuclear, ETSEIB Universitat Politècnica de Catalunya, Diagonal, 647 08028 Barcelona, Spain;* [b]*Liquid Crystals Institute, Kent State University, Kent, OH 44242-0001, USA;* [c]*Departamento de Física Aplicada II, Facultad de Ciencias, Universidad del País Vasco, Apartado 644, E-48080 Bilbao, Spain*

(Received 14 February 2008; final form 10 April 2008)

Measurements of pressure, molar volume and specific heat as functions of temperature in the isotropic (I) phase as well as in the smectic A (SmA) and nematic (N) mesophases of some alkyloxycyanobiphenyl compounds (*n*OCB, $n=6$–10) were carried out using differential thermal analysis under pressure, densitometry, X-ray powder diffraction and modulated differential scanning calorimetry. Thermodynamic properties, such as latent heats and volume jumps at the different phase transitions, were determined. The coherence of this whole set of data was tested using pressure–temperature data through the slopes associated to their phase transitions, extrapolated at normal pressure in the light of the Clausius–Clapeyron equation.

Keywords: Clausius–Clapeyron equation; molar volume; odd–even effect; pressure–temperature diagrams

1. Introduction

Experimental determinations of the thermodynamic properties of materials provide further knowledge not only of their fundamental behaviour, but also of their applications in several fields of science and technology.

One type of material for which thermodynamic properties have been and are widely investigated is the so-called calamitic liquid crystals. These materials are constituted by rod-like organic molecules with anisotropic molecular structures, mostly with strong dipole moments and easily polarisable substituents. They exhibit, between the anisotropic ordered crystalline state (Cr) and the isotropic liquid state (I), a variety of phases (mesophases), defined by the orientational and spatial ordering of the molecules, the symmetries and mechanical properties of which are intermediate between those of an isotropic liquid and the ordered crystal. Two of the more common mesophases are the nematic (N) and the smectic A (SmA) phases. In both phases, the long axes of the rod-like molecules are oriented along a preferred direction in such a way that in the N phase their centres of mass are randomly positioned, whereas in the SmA mesophase, the molecules are additionally ordered in layers perpendicular to their orientation.

One type of calamitic liquid crystal is the so-called alkoxycyanobiphenyls, *n*OCB (*n* being the number of carbon atoms in the alkoxy chain), that exhibit one or two mesomorphic phases, with the phase sequence strongly influenced by the effect of pressure.

From the technical point of view, *n*OCB materials have interesting applications owing to their characteristic photophysical (*1*) and electro-optical (*2*) properties. Their applicability ranges from the engineering of liquid crystal devices to the more recently evidenced possibility of infiltration of liquid crystals in several kinds of porous matrices, thus opening the door to novel future applications such as tuneable photonic crystal lasers (*3*), waveguides (*4*) or optical limiters (*4*). But apart from their technical applications, the materials are appropriate for testing the different theoretical proposals about phase transitions (*5–21*).

The goal of the present paper is to present a thermodynamic description, as complete as possible, concerning all the first-order phase transitions exhibited by 6OCB, 7OCB, 8OCB, 9OCB and 10OCB liquid crystals at normal pressure. In order to achieve this purpose, the magnitudes involved in the Clausius–Clapeyron equation must be accurately obtained from the different experimental techniques: the slope of pressure–temperature phase diagrams, the latent heat, the jump in molar volume and the corresponding transition temperature for the analysed phase transitions. It should be noted that some information about these magnitudes exists in the literature, but this information is far from being complete and homogeneous. Some thermodynamic data have been previously published elsewhere by our research group as a consequence of studies about the critical behaviour and the effect of geometries more restrictive than bulk on the above mentioned

---

*Corresponding author. Email: josep.salud@upc.edu

ISSN 0267-8292 print/ISSN 1366-5855 online

DOI: 10.1080/02678290802120273
http://www.informaworld.com

transitions (*10, 15–21*), with the exception of 6OCB, results for which will appear in a future paper. On the other hand, and as far as we know, experimental information does not appear to exist in the literature about the pressure–temperature phase diagram of 7OCB.

The paper is organised as follows. The experimental details are described in section 2. Pressure–temperature, specific heat as well as volumetric studies of the first-order phase transitions are discussed and presented in section 3. Finally, in section 4, an overall discussion along with a summary of the main conclusions is made.

2. Experimental details

Materials

The materials studied were the mesogenic compounds 6OCB, 7OCB, 8OCB, 9OCB and 10OCB, which were synthesised by Professor Dabrowsky at the Institute of Chemistry, Military University of Technology, Warsaw, Poland. The purity was stated to be higher than 99.9%, and no further purification was made.

Experimental techniques

Thermal analysis at normal pressure.

Thermal analysis at normal pressure was performed using a commercial differential scanning calorimeter (TA Instruments DSC 2920) equipped with a cryogenic cooling accessory (123 K), working in modulated mode to obtain the specific heat data. In such a mode, the technique is also suitable for determinations of latent heats of first-order transitions, whether they are weak or not. To do so, a special calibration procedure was performed, in which very precise latent heat data measured from other homologous compounds through adiabatic calorimetry have been considered.

The measurements consisted in heating the samples from smectic phase at $0.01\,\mathrm{K\,min^{-1}}$, with a modulation temperature amplitude of ± 0.035 K and a period of 25 s. The sample masses (chosen between 1–2 mg) were selected to ensure a uniform thin layer within the Al pans. The specific heat calibration was performed using pure synthetic sapphire. Extensive details of the experimental set-up are provided elsewhere (*15, 19*).

Thermal analysis at high pressure.

The thermal behaviour of the compounds at high pressures was examined by using a homemade differential thermal analysis (DTA) apparatus (*22*), which is able to work up to 400 MPa in the range of 300–530 K, with a methanol:ethanol mixture (4:1 by volume) used as the pressure-transmitting liquid. DTA peaks were generated at heating rates of 1–$2\,\mathrm{K\,min^{-1}}$. Samples (of about 20 mg) were encapsulated in indium cells because indium is a soft material that favours the pressure transmission between the medium and the sample. The device was calibrated in temperature with bromotrichloroethane ($CBrCl_3$) in the interval of analysed pressures. Transition temperatures were determined as the onset temperatures of the corresponding endothermic peaks in the thermograms.

X-ray powder diffraction.

High-resolution X-ray powder diffraction patterns using the Debye–Scherrer geometry and transmission mode were recorded with a horizontally mounted INEL cylindrical position-sensitive detector (CPS-120) made of 4096 channels (angular step, $2\theta \approx 0.029°$). Monochromatic Cu $K\alpha_1$ ($\lambda = 1.54056$ Å) radiation was selected by means of an asymmetrically focusing incident beam in a curved quartz monochromator. The generator power was set to 35 kV and 35 mA.

The samples were introduced into 0.5 mm diameter Lindemann glass capillaries and were rotated around the θ axis during the experiments. External calibration using the cubic phase $Na_2Ca_3Al_2F_4$ was performed to convert channels to 2θ degrees by means of cubic spline fittings in order to correct the deviation from angular linearity in PSD. The peak positions were determined after pseudo–Voigt fittings in the standard measurements by using the PEAKOC application from Difractinel software (*23*).

Molar volume measurements at atmospheric pressure.

Molar volume measurements at normal pressure were carried out using an Anton Paar DMA-5000 density meter coupled to a homemade filling syringe system. The sample temperature was controlled with a precision of ± 1 mK and the acquisitions of data were made by steps of 0.01 K in the region of the phase transitions and 0.02 K otherwise, with stabilisation period of 300 s. The device was initially calibrated by using bidistilled water and octylcyanobiphenyl (8CB), for which high-resolution density data from dilatometric measurements can be found in the literature (*24, 25*).

3. Results and discussion

Thermal characterization at atmospheric pressure

Thermal measurements, not only in *n*OCB, but also in some of their binary mixtures (*10, 15, 18, 19*) as a result of experimental determinations of the critical behaviour at their mesophase–mesophase or mesophase–isotropic phase transitions, have already been obtained.

In order to obtain valuable information about phase transitions at atmospheric pressure in the studied compounds, as already mentioned, the modulated differential scanning calorimetry (MDSC) technique or the widely used ac calorimetry (*15, 26–28*) has been proved to be very precise in distinguishing the order of phase transitions through phase shift changes. Additionally, the MDSC technique, unlike ac calorimetry, provides the ability to obtain latent heats, ΔH, in weakly first-order phase transitions. For that purpose, in a given experiment it is convenient to define (*18*)

$$\Delta H_{TOT} = \Delta H + \int \Delta C_p dT, \tag{1}$$

where the second term is the pre-transitional fluctuation contribution [$\Delta C_p \equiv C_p - C_p$(background) is the excess specific heat due to the change in ordering that is associated with the transition]. If a phase transition is of second order, the latent heat ΔH vanishes. On the other hand, for strongly first-order phase transitions, the latent heat ΔH is much more higher than the integrated pre-transitional fluctuation contribution ($\int \Delta C_p dT$) in such a way that this term is assumed to be negligible and the observed total enthalpy, ΔH_{TOT}, can be identified with the latent heat, ΔH. This is the case of those transitions referred to as crystal Cr-mesophase in the present study. However, for weakly first-order phase transitions, such as the mesophase–isotropic (I) transitions and the SmA–N transition in 9OCB, both terms in equation (1) must be considered. The latent heat, ΔH, can be obtained from the MDSC technique by means of a special calibration.

In Table 1, the results concerning the latent heats and transition temperatures for all the studied compounds are collected. Latent heats corresponding to Cr-to-mesophase exhibit values two orders higher than those from N-I transitions, whereas that corresponding to the SmA-to-I phase transition (in 10OCB) exhibits an intermediate value. This behaviour is in agreement with what is observed for the volume jump data.

Thermal characterization under pressure

To the best of our knowledge, for all the studied *n*OCB compounds (n=6–10), with the exception of 7OCB, exist experimental determinations of their thermal behaviour under pressure (*29–31*). However, we present here new determinations of their pressure–temperature phase diagrams enlarged up to 2.5–2.8×10^2 MPa in order to perform a complete thermodynamic treatment of their different phase transitions. As an example, in Figure 1 typical DTA traces for 6OCB at 40 MPa and 140 MPa are displayed, showing the Cr–N and N–I phase transitions, respectively, and this behaviour is maintained over the whole experimental pressure range.

Table 1. Enthalpies (ΔH), volume changes (ΔV) and phase transition temperatures (T_{tr}) for *n*OCB compounds (n=6–10).

Compound	Transition	ΔH/kJ mol^{-1}	T_{tr}/K	ΔV/cm^3 mol^{-1}
6OCB	Cr–N	23.02	331.11	21.70
	N–I	0.31	349.54	0.28
7OCB	Cr–N	29.20	327.22	21.51
	N–I	0.33	347.31	0.29
8OCB	Cr–SmA	26.65	327.68	24.19
	SmA–N	<0.03	340.37	–
	N–I	0.49	353.39	0.42
9OCB	Cr–SmA	39.84	336.95	31.62
	SmA–N	0.16	351.08	0.10
	N–I	0.84	353.22	0.71
10OCB	Cr–SmA	32.5	332.65	26.83
	SmA–I	2.52	357.02	2.35

Figure 2 shows the phase behaviour of the nOCB series between 320 and 440 K, where empty symbol curves are the transition lines fitted by polynomials to the experimental data from literature (*29–31*). Full symbols correspond to experimental determinations obtained in this work and full symbol curves are

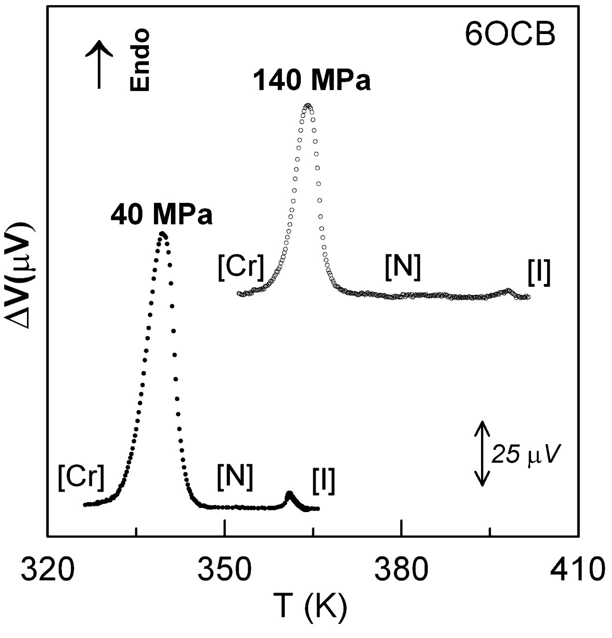

Figure 1. DTA curves of 6OCB at 40 MPa and 140 MPa for a heating rate of 2 K min^{-1}.

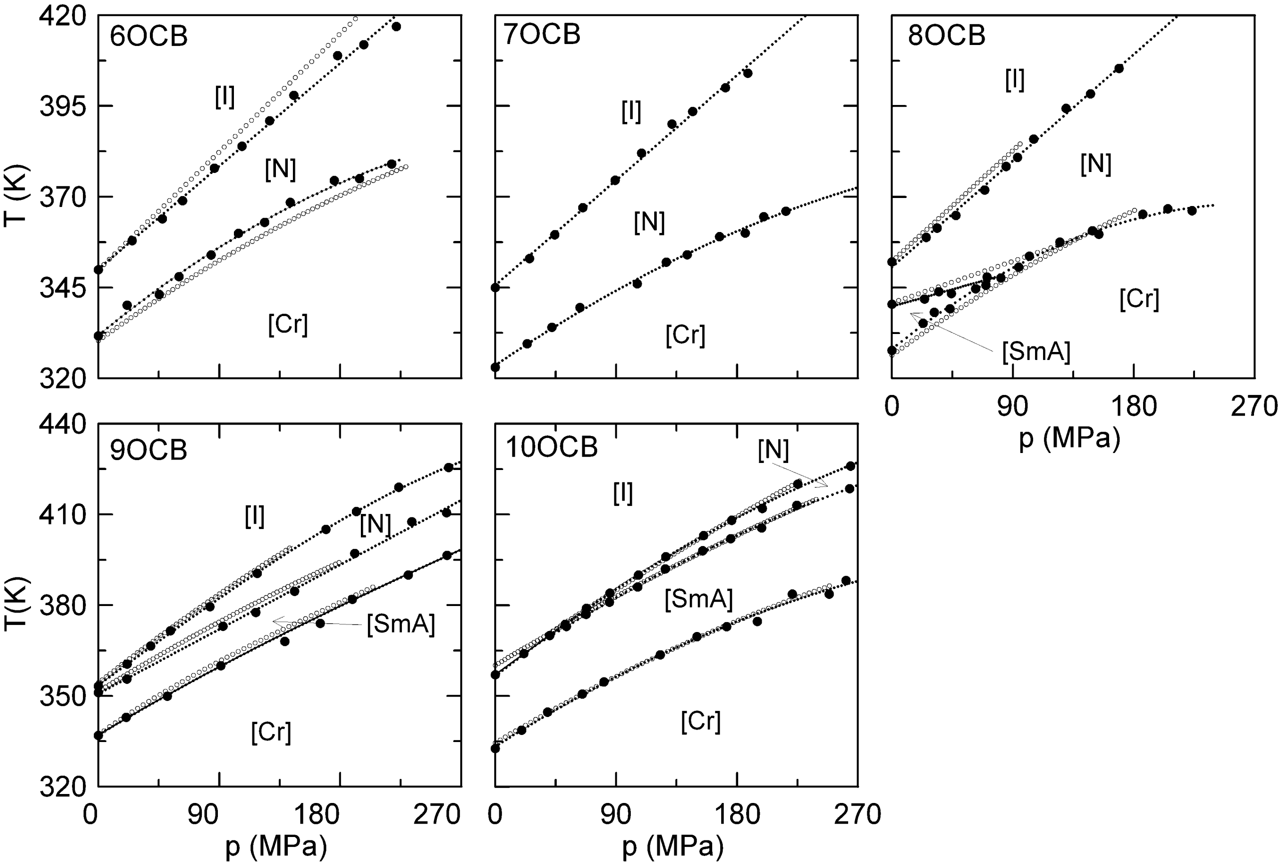

Figure 2. Temperature–pressure phase diagrams (full symbols) for 6OCB, 7OCB, 8OCB, 9OCB and 10OCB. Full symbol curves are polynomial fittings to experimental data. Empty symbol curves are experimental data from the literature (26–28).

referred to polynomial fittings. There are two striking characteristics of these diagrams. On the one hand, the nematic range, defined by the temperature interval in which the nematic phase exists at a given pressure, becomes somewhat broader with increasing pressure, this phenomenon being usual for conventional liquid crystals (*32–34*).

On the other hand, there is evidence of an opposite effect on the phase behaviour with increasing pressure: whereas the SmA phase disappears in the 8OCB starting at pressures above 120 MPa, a nematic phase is induced in 10OCB for pressures above 40 MPa. From the continuous curves it is possible to obtain their slopes, *dT*/*dp*, at atmospheric pressure, which will be used later in order to establish the coherence of all the thermal data concerning the studied compounds. The values thus obtained are gathered in Table 2.

Molar volume behaviour

Although some published experimental data (*35–42*) exists concerning the molar volume of *n*OCB compounds, mainly in the mesophases, new and complementary data have been obtained in order to determine the molar volume jumps at the different first-order phase transitions.

Table 2. Slope of the two-phase coexistence lines in the pressure–temperature diagram and the term $\Delta H/T\Delta V$, both at atmospheric pressure, where ΔH is the latent heat in J mol^{-1}, ΔV the jump in molar volume in m^3 mol^{-1} and T the transition temperature in K corresponding to the first-order phase transitions for 6OCB, 7OCB, 8OCB, 9OCB and 10OCB.

Compound	Transition	$\left(\frac{dp}{dT}\right)_{p\to 0}\times 10^6 / \mathrm{Pa\,K^{-1}}$	$\frac{\Delta H}{T\Delta V}\times 10^6 / \mathrm{Pa\,K^{-1}}$
6OCB	Cr–N	3.28	3.20
	N–I	3.14	3.16
7OCB	Cr–N	3.95	4.15
	N–I	3.11	3.23
8OCB	Cr–SmA	3.34	3.36
	N–I	3.26	3.27
9OCB	Cr–SmA	3.74	3.74
	SmA–N	4.19	4.56
	N–I	3.24	3.37
10OCB	Cr–SmA	3.53	3.64
	SmA–I	3.12	3.00

As far as crystal phases are concerned, X-ray powder diffraction measurements have been carried out on heating the samples. The corresponding X-ray powder diffraction profiles were obtained at several temperatures. To do so, literature information was used to obtain crystal symmetry and lattice parameters (*43–47*). Lattice parameter refinements to obtain molar volumes were made by using the AFMAIL program (*48*).

As for the mesophases (either SmA or N) and for the isotropic phase, the molar volume as a function of temperature was obtained from density measurements. The results at atmospheric pressure as a function of temperature are displayed in Figure 3. In

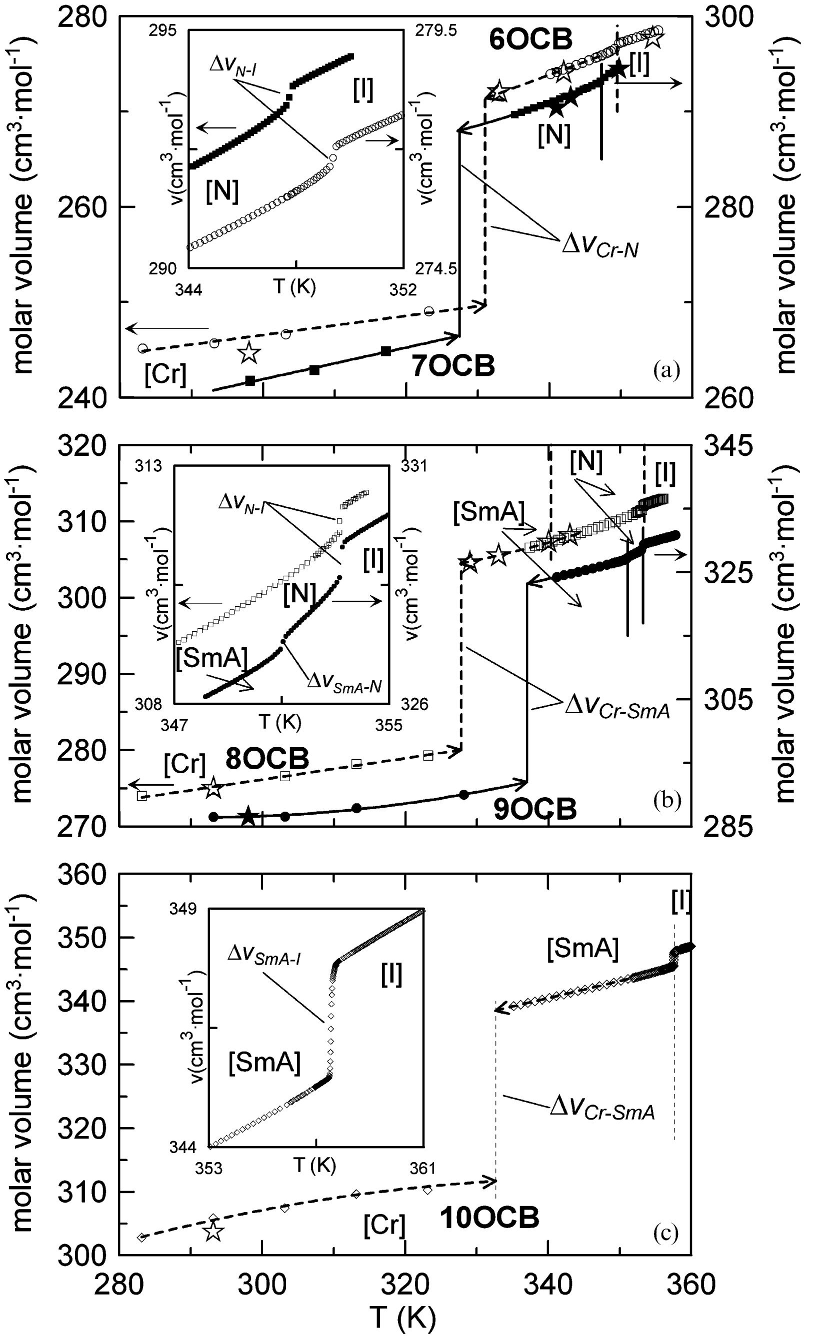

Figure 3. Molar volume as a function of temperature for the crystal, mesogenic (SmA and/or N) and I phases for (a) 6OCB (open circles) and 7OCB (filled squares), (b) 8OCB (empty squares) and 9OCB (full circles) and (c) 10OCB (empty diamonds). Filled and empty star symbols are some literature data for the crystal and mesophases.

such a figure, volume jumps at the different N-to-I phase transitions are enlarged in the insets of figures 3 A and 3 B. In the latter, additionally, the volume jump corresponding to the SmA-N phase transition of 9OCB, which has been recently proved to be first order (*16*), is also displayed. On the other hand, the inset of figure 3 C displays the SmA-I phase transition of 10OCB. Furthermore, and as a comparison, experimental molar volume data from literature are shown, not only in the crystal phase (*43–47*), but also in the mesophases. In the first case, the agreement with our measurements is evident, although it must be remarked that for the 7OCB the corresponding value has not been included because it was obtained at a temperature out of the range shown in figure 3 A. Concerning the mesophase literature data (*36, 38–40, 42*), as can be seen from figure 3, there seems to be a reasonable agreement between the data and the results reported here, with the exception of 9OCB and 10OCB. The literature data concerning to these compounds do not appear in the figure because they are remarkably different, probably as a result of the experimental methodology (*16, 36, 40*) used.

As for the SmA-to-N phase transition of 8OCB, no appreciable volume jump (ΔV) has been detected as it is expected due to its second order character in nature (*10, 41*). Our volume jump data are summarised in Table 1. It must be remarked that the ΔV values for the crystal-mesophase transitions are about two orders of magnitude higher than those corresponding to the mesophase-to-mesophase or mesophase-isotropic phase transitions.

4. Overall discussion and concluding remarks

It is well known that the so called Clausius–Clapeyron equation,

$$\frac{dp}{dT}=\frac{\Delta H}{T\Delta V}, \tag{2}$$

holds for the pressure–temperature curves belonging to a first-order phase transition, where dp/dT is the slope of such curves, and ΔH, ΔV and T are, respectively, the latent heat, the jump in molar volume and the temperature of the phase transition. By means of this equation it is possible to test the overall coherence of the corresponding experimental values of these magnitudes, which have been collated in section 3 for the *n*OCB series of liquid crystals (n=6–10). For that purpose, in Figure 4 the left hand part of the Clausius–Clapeyron equation is plotted against the right hand one. The dashed diagonal line in the figure represents the exact matching among the physical magnitudes (dp/dT, ΔH, T and ΔV) according to equation (2). The matching or not between the experimental data and this master line reveals their coherence and, to assist the reader in such a comparison, estimated experimental error bars are included in Figure 4. The error quoted for dp/dT data arises from the fitting procedure of experimental data, whereas the other errors have been estimated according to the methodology used. Experimental points corresponding to Cr-mesophase transitions are represented by means of full symbols and although they seem to be well-distributed along the master line, they do not exhibit a regular correspondence with the chain length (n) in the *n*OCB series. As for the mesophase-I phase transitions, the data are represented by empty symbols and are located onto the master line but in the left-lower side in a more or less random fashion in relation to the chain length, (n). Additionally, the only datum corresponding to first-order SmA-N phase transition in 9OCB, represented by an empty-full cross, is located at the top right side of Figure 4. Its matching with the master line is less evident despite the error bars and it is likely due to its very weak first-order character in concordance with the extremely low values in latent heat and molar volume jump in the transition.

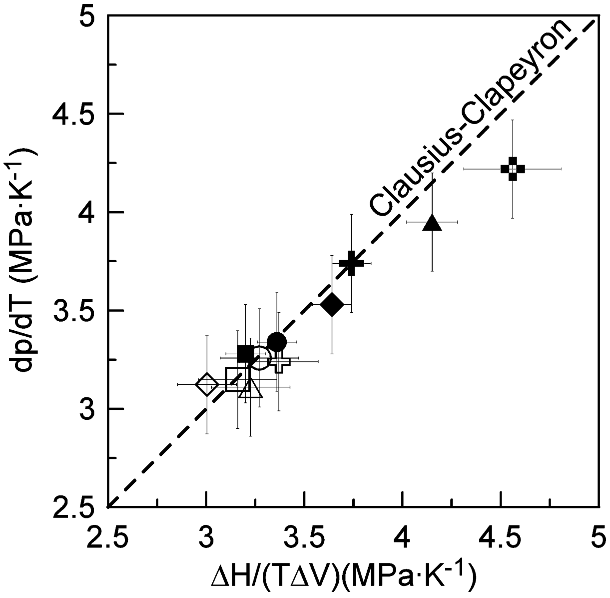

Figure 4. Slope, dp/dT at normal pressure, versus $\Delta H/T\Delta V$ for the first-order phase transitions in the *n*OCB (n=6–10) liquid crystals. ■ Cr–N 6OCB, □ N–I 6OCB, ▲ Cr–N 7OCB, △ N–I 7OCB, ● Cr–SmA 8OCB, ○ N–I 8OCB, ✚ Cr–SmA 9OCB, ✜ SmA–N 9OCB, ✙ N–I 9OCB, ◆ Cr–SmA 10OCB, ◇ SmA–I 10OCB. The diagonal dashed line represents the Clausius–Clapeyron equation.

To explain the apparent random distribution of data in Figure 4 along the master line, it is important to remember that, in general, materials belonging to homologous series of low molar mass mesogens exhibit transitional properties (such as, for example, temperature, enthalpy or entropy, order parameter and thermal conductivity) that are strongly dependent on the length of the alkyl tail (*n*), in such a way that they can exhibit on average a bit higher/lower values in even-numbered lengths than in odd ones, i.e. what is known as the odd–even effect (*49–52*). From a theoretical point of view (*53, 54*), the odd–even effect, depending on the physical magnitude, can be attributed to enthalpic and/or steric factors, among others.

In Figure 5, the slope *dp*/*dT* at normal pressure for the Cr-to-mesophase as well as for the mesophase-I phase transitions is presented as a function of the number *n* of carbon atoms in the alkyl chain of the *n*OCB series (*n*=6–10). A pronounced odd–even effect is observed for *dp*/*dT* at normal pressure at the Cr-mesophase phase transitions. Nevertheless, it is important to realise that the Cr-mesophase transition temperatures for the same compounds behave in an irregular manner. In the inset of figure 5 A, both the latent heat (ΔH) and $T\Delta V$ for the same phase transitions are plotted as a function of *n* for the *n*OCBs. The latent heat shows a

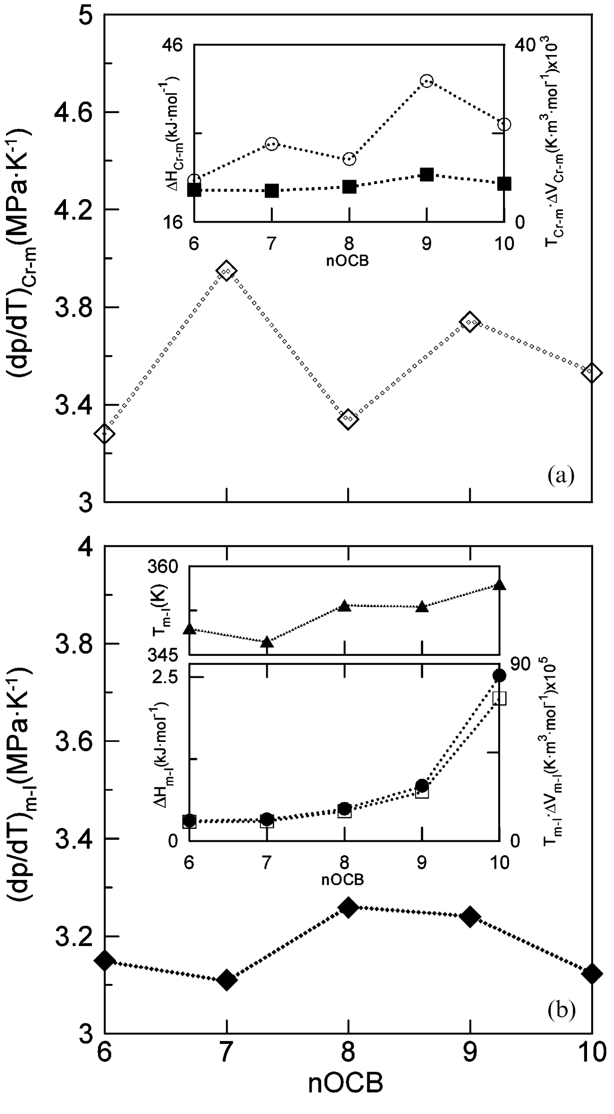

Figure 5. Slope, *dp*/*dT* at normal pressure, as a function of the number *n* of carbon atoms in the alkoxy chain length of the *n*OCB homologous series (*n*=6–10) referred to the (a) crystal–mesophase and (b) mesophase–isotropic phase transitions. The inset in (a) represents the dependence of the enthalpy, ΔH (open circles), and the term $T\Delta V$ (filled squares) at the crystal–mesophase phase transitions as a function of *n*. The top inset in (b) represents the evolution of the transition temperatures at the mesophase–isotropic phase transitions as a function of *n*. The bottom inset in (b) represents the dependence of the enthalpy, ΔH (filled circles), and the term $T\Delta V$ (open squares) at the mesophase–isotropic phase transitions as a function of *n*.

similar pronounced alternation as *dp*/*dT*, whereas the steric factors via $T\Delta V$ seem to be only responsible of the attenuation in the odd–even effect in *dp*/*dT*. The apparent lack of odd–even effect in the Cr-mesophase transition temperatures in the *n*OCB series is similar to the evolution in the molar volume jump along the series (see Table 1).

From Figure 5 B, a less pronounced odd–even effect seems to be present for *dp*/*dT* at normal pressure for the mesophase-I phase transition, with the exception of the SmA-I transition ($n=10$). In such a case, neither enthalpic (latent heat) nor steric ($T\Delta V$) effects seem to be responsible of the slight attenuation presented in *dp*/*dT*, as can be seen in the bottom inset of Figure 5 B. Nevertheless, from the top-inset of the same figure, it can be concluded that the observed odd–even effect in the mesophase-I transition temperatures is similar to that observed for *dp*/*dT* at normal pressure, at least, up to $n=9$.

In summary, an overall analysis concerning the first-order crystal-mesophase and mesophase-I phase transitions in *n*OCB ($n=6$–10) liquid crystals has been carried out by means of experimental determinations of the magnitudes involved in the Clausius–Clapeyron equation. It seems evident that all data concerning the involved phase transitions match up the theoretical Clausius–Clapeyron equation but in an irregular correspondence with the alkoxy chain length of the compounds. Figure 5 clearly shows this fact in such way that an odd–even effect in *dp*/*dT* at normal pressure must be reported for the crystal-mesophase and in a lesser extent for the mesophase-I phase transitions. The analysis of the data seems to reflect a different role played by the enthalpic or steric factors in the crystal-to-mesophase transitions in comparison with the mesophase-I phase ones.

Acknowledgements

The authors wish to express their gratitude for the financial support from the MCYT (project FIS2005-00975) and the MEC (project MAT2006-13571-C02-02) of Spanish Government, the DURSI (grant 2005SGR-00535) from the Generalitat de Catalunya's Government and the Gobierno Vasco (grant IT-484-07).

References

(1) Tamai N.; Yamazaki I. *Chem. Phys. Lett.* **1984**, *104*, 485–488.
(2) Kirton J.; Raynes E.P. *Endeavour* **1973**, *32*, 71–75.
(3) Yablonovith E. *Nature* **1999**, *401*, 539–541.
(4) Leonard S.W.; Mondia J.P.; van Driel H.M.N.; Toader O.; John S.; Busch K.; Birner A.; Gösele U. *Phys. Rev. B* **2000**, *61*, R2389–R2392.
(5) Kobayashi K. *Phys. Lett. A* **1970**, *31*, 125–127.
(6) McMillan W.L. *Phys. Rev. A* **1971**, *4*, 1238–1246.
(7) de Gennes P.G. *The Physics of Liquid Crystals*; Oxford Science Publications: Oxford, 1994.
(8) Thoen J.; Marynissen H.; van Dael W. *Phys. Rev. Lett.* **1984**, *52*, 204–207.
(9) Thoen J.; Marynissen H.; van Dael W. *Phys. Rev. A* **1982**, *26*, 2886–2905.
(10) Sied M.B.; López D.O.; Tamarit J.L.; Barrio M. *Liq. Cryst.* **2002**, *29*, 57–66.
(11) Zywocinski A.; Wieczorek S.A. *J. Phys. Chem. B* **1997**, *101*, 6870–6976.
(12) Sandmann M.; Würflinger A. *Z. Naturf. A* **1998**, *53*, 787–792.
(13) Oweimreen G.A.; Morsy M.A. *Thermochim. Acta* **2000**, *346*, 37–47.
(14) Oweimreen G.A. *J. Phys. Chem. B* **2001**, *105*, 8417–8419.
(15) Sied M.B.; Salud J.; López D.O.; Barrio M.; Tamarit J.L. *Phys. Chem. Chem. Phys.* **2002**, *4*, 2587–2593.
(16) Cusmin P.; de la Fuente M.R.; Salud J.; Pérez-Jubindo M.A.; Diez-Berart S.; López D.O. *J. Phys. Chem. B* **2007**, *111*, 8974–8984.
(17) Sied M.B.; Salud J.; López D.O.; Allouchi H.; Diez S.; Tamarit J.L. *J. Phys. Chem. B* **2003**, *107*, 7820–7829.
(18) Sied M.B.; Diez S.; Salud J.; López D.O.; Cusmin P.; Tamarit J.L.; Barrio M. *J. Phys. Chem. B* **2005**, *109*, 16284–16289.
(19) Cusmin P.; Salud J.; López D.O.; de la Fuente M.R.; Diez S.; Pérez-Jubindo M.A.; Barrio M.; Tamarit J.L. *J. Phys. Chem. B* **2006**, *110*, 26194–26203.
(20) Diez S.; López D.O.; de la Fuente M.R.; Pérez-Jubindo M.A.; Salud J.; Tamarit J.L. *J. Phys. Chem. B* **2005**, *109*, 23209–23217.
(21) Sied M.B., Ph.D. Thesis, Politècnica de Catalunya University, Barcelona, 2005.
(22) Pizarro A. *PFC*; Universitat Politècnica de Catalunya, 2004.
(23) Masson A.; Ramponi A. *PEAKOC Program*; Laboratoire de Matériaux Céramiques et Traitements de Surfaces, CNRS-ENSCI: Limoges, France, 1996.
(24) Zywocinski A. *J. phys. Chem. B* **2003**, *107*, 9491–9497.
(25) Ziwocinski A.; Wieczorek S.A. *J. Phys. Chem. B* **1997**, *101*, 6970–6976.
(26) Garland C.W. *Thermochim. Acta* **1985**, *88*, 127–142.
(27) Iannachhione G.S.; Finotello D. *Phys. Rev. E* **1994**, *50*, 4780–4795.
(28) Quian S.; Iannachhione G.S.; Finotello D. *Phys. Rev. E* **1998**, *57*, 4305–4315.
(29) Krombach R.; Schneider G.M. *Thermochim. Acta* **1994**, *231*, 169–175.
(30) Brückert T.; Urban S.; Würflinger A. *Ber. Bunsenges. Phys. Chem.* **1996**, *100*, 1133–1137.
(31) Schneider G.M. *Thermochim. Acta* **1985**, *88*, 17–34.
(32) Kuss E. *Mol. Cryst. Liq. Cryst.* **1978**, *47*, 71–83.
(33) Spratte W.; Schneider G.M. *Ber. Bunsenges. Phys. Chem.* **1976**, *80*, 886–891.
(34) Urban S.; Massalska-Arodz M.; Würflinger A.; Dabrowski R. *Liq. Cryst.* **2003**, *30*, 313–318.
(35) Venkatacharyulu P.; Gupta A.V.N.; Rao J.V.; Prasad K.S.R.; Prasad N.V.L.N. *Cryst. Res. Technol.* **1989**, *24*, 835–844.
(36) Sen S.; Brahma P.; Roy S.K.; Mukherjee D.K.; Roy S.B. *Mol. Cryst. Liq. Cryst.* **1983**, *100*, 327–340.
(37) Czupyrinski K.; Dabrowski R.; Baran J.; Zywocinski A.; Przedmojski J. *J. Phys., Paris* **1986**, *47*, 1577–1585.

(38) Burmistrov V.A.; Zav'yalov A.V.; Novikov I.V.; Kuvshinova S.A.; Aleksandrinskii V.V. *Rus. J. Phys. Chem.* **2005**, *79*, 130–132.

(39) Ghanadzadeh A.; Ghanadzadeh H.; Khoshroo N. *J. Mol. Liq.* **2001**, *94*, 37–49.

(40) Zywocinski A. *J. Phys. Chem. B* **1999**, *103*, 3087–3092.

(41) Zywocinski A.; Wieczorek S.A.; Stecki J. *Phys. Rev. A* **1987**, *36*, 1901–1907.

(42) Mitra M.; Gupta S.; Paul R.; Paul S. *Mol. Cryst. Liq. Cryst.* **1991**, *199*, 257–266.

(43) Hori K.; Koma Y.; Uchida A.; Ohashi Y. *Mol. Cryst. Liq. Cryst.* **1993**, *225*, 15–22.

(44) Hori K.; Koma Y.; Kurosaki M.; Itoh K.; Uekusa H.; Takenaka Y.; Ohashi Y. *Bull. Chem. Soc. Japan* **1996**, *69*, 891–897.

(45) Hori K.; Iwai Y.; Yano M.; Orihara-Furukawa R.; Tominaga Y.; Nishibori F.; Takata M.; Sakata M.; Kato K. *Bull. Chem. Soc. Japan* **2005**, *78*, 1223–1229.

(46) Hori K.; Wu H. *Liq. Cryst.* **1999**, *26*, 37–43.

(47) Das M.K.; Paul S.; Paul R. *Mol. Cryst. Liq. Cryst.* **1995**, *264*, 89–98.

(48) Rodríguez-Carvajal J. *AFMAIL program*; Laboratoire Léon Brillouin, CEA-CNRS: Gif-sur-Yvette, France, 1985.

(49) Imrie C.T.; Karasz F.E.; Attard G.S. *Macromolecules* **1993**, *26*, 3803–3820.

(50) Imrie C.T.; Lukhurst G.R. *J. Mater. Chem.* **1998**, *8*, 1339–1343.

(51) Marinelli M.; Mercuri F.; Zammit U.; Scuderi F. *Phys. Rev. E* **1998**, *58*, 5860–5866.

(52) Bielejewska N.; Chrzumnicka E.; Mykowska E.; Przybylski R.; Szybowicz M.; Wladysiak K.; Bauman D. *Acta Phys. Polon.* **2006**, *110*, 777–793.

(53) Marcelja S. *J. Chem. Phys.* **1974**, *60*, 3599–3604.

(54) Ilk Carpar M.; Cebe E. *J. Comput. Chem.* **2007**, *28*, 2140–2146.